Published in: Developments in Strategic Ceramic Materials: Ceramic Engineering and Science Proceedings Volume 36 Issue 8, page 169-177 (2016) – Wiley-VCH, ISBN: 978-1-119-21173-0

DOPING OF CeO_2 AS A TUNABLE BUFFER LAYER FOR COATED SUPERCONDUCTORS: A DFT STUDY OF MECHANICAL AND ELECTRONIC PROPERTIES

Danny E. P. Vanpoucke
Center for Molecular Modeling, Ghent University, Technologiepark 903, 9052 Zwijnaarde, Belgium

ABSTRACT

In layered ceramic superconductor architectures, CeO_2 buffer layers are known to form micro cracks during the fabrication process. To prevent this crack formation, doping of the CeO_2 layer has been suggested. In this theoretical study, the influence of dopants (both tetravalent and aliovalent) on the mechanical and structural properties of CeO_2 is investigated by means of density functional theory. Group IVa and IVb dopants show clearly distinct stability, with the former favouring interface and surface doping, while the latter favour uniform bulk doping. This behaviour is linked to the dopant electronic structure. The presence of charge compensating vacancies is shown to complicate the mechanical and structural picture for aliovalent dopants. We find that the vacancies often counteract the dopant modifications of the host material. In contrast, all dopants show an inverse relation between the bulk modulus and thermal expansion coefficient, independent of their valency and the presence of oxygen vacancies. Based on the study of these idealized systems, new dopants are suggested for applications.

INTRODUCTION

A major industrial application in the field of superconductivity is the production of superconducting wires, which in turn can be used to produce coils for superconducting magnets. In the development of high temperature superconducting wires and components, $YBa_2Cu_3O_{7-d}$ remains one of the most important materials. Because it is a ceramic material, it is brittle by nature, making it ill-suited for wiredrawing. To produce an industrial scale wire with the required flexibility one can use a coated superconductor architecture instead. In such architecture, a thin film of the superconductor is deposited on a metal wire or tape, combining the flexibility of the metal substrate with the superconducting properties of the thin film. To prevent metal atoms of diffusing from the substrate into the superconductor, and thus destroying its superconducting properties, one or more buffer layers are deposited between the substrate and the thin film superconductor. Recently, cerium oxide (CeO_2) has been used as such a buffer layer;[1,2,3,4,5] however, the layer thickness of these buffer layers is limited by the formation of cracks during deposition,[2,4] limiting their interest for industrial applications. In addition, economic factors demand the entire architecture to contain as few layers as possible this means that the individual buffer layers need to be a thick as possible. As such it is of great interest to increase the layer thickness before the onset of crackformation. The formation of these microcracks has been linked to internal stress, and metal doping has been suggested as a means of reducing this internal stress, by alleviating the lattice mismatch and mismatch of the thermal expansion coefficients between the different layers.[4]

In this work, we investigate the influence of dopants on the structural and mechanical properties of CeO_2 using density functional theory (DFT) calculations. The introduction of a dopant gives rise to three separate modifications of the system, each having its influence on the properties of CeO_2: (1) Different electronic structure of the dopant and cerium, (2) different oxidation state of the dopant (aliovalent dopants) and cerium, and (3) the formation of charge compensating oxygen vacancies in the case of aliovalent dopants.

To have a clear understanding of the influence dopants have on the properties of CeO_2, it is important to separate the different contributions; i.e. to distinguish between the consequences

of doping (both the effect of the different electronic structure in case of isovalent dopants, and the effect of the oxidation state in case of aliovalent dopants) and subsequently those of the introduced charge compensating vacancies. Theoretical calculations are ideally suited to distinguish between these different contributions, since they allow the system under study to be tailored to these specific needs. In addition to the prediction of new possible dopants, they also provide ways to estimate required dopant concentrations for tuning applications (e.g. lattice parameter matching).

COMPUTATIONAL METHODS

DFT calculations are performed using the projector augmented wave (PAW) method as implemented in the Vienna ab initio Package (VASP) program.[6,7] The GGA functional as constructed by Perdew, Burke and Ernzerhof (PBE) is used to model the exchange and correlation behavior of the electrons.[8] The plane wave kinetic energy cutoff is set to 500 eV. To optimize the structures, a conjugate gradient method is used. During relaxation both atom positions and cell-geometry are allowed to change simultaneously. The convergence criterion is set to the difference in energy between subsequent steps becoming smaller than 1.0×10^{-6} eV. Because this work focusses on general trends in the properties of doped CeO_2 as a function of dopant concentration, we assume the dopants to be distributed homogeneously in an ordered fashion. This allows for the investigation of a wide range of concentrations going from about 3% up to 25%. Figure 1 shows the conventional 12-atom cubic unit cell of CeO_2 with a single dopant (dopant concentration = 25%).

The thermal expansion coefficient is calculated as the numerical derivative of V(T) data, which is obtained from the minimization of the thermal non-equilibrium Gibbs function. The latter is calculated using the quasi-harmonic Debye approximation, and is implemented as a module in our in-house developed HIVE code.[9,10] The bulk modulus is obtained from fitting E(V) data from fixed volume calculations to the Rose-Vinet equation of state.[11] Hirshfeld-I charges are calculated from the electron density distributions.[12,13,14] The required atom-centered spherical integration make use of Lebedev-Laikov grids of 1202 grid-points combined with a logarithmic radial grid.[15]

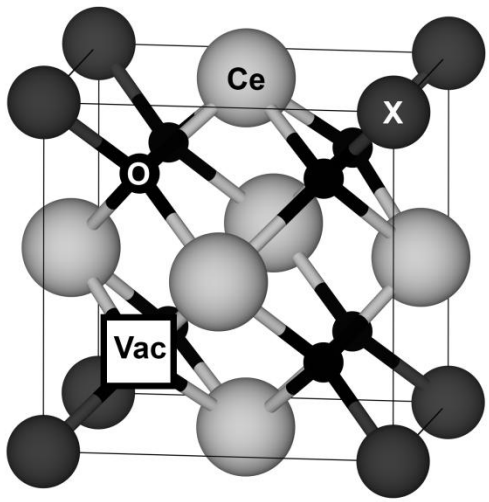

Figure 1: Ball-and-stick representation of $Ce_{0.75}X_{0.25}O_2$.The position of the oxygen vacancy for systems containing vacancies is indicated.

RESULTS AND DISCUSSION

Tetravalent Dopants

Because cerium is tetravalent in cerium oxide, we focus on the group IV elements as dopants in a first step. The stability of the dopants is investigated through the comparison of their defect formation energies calculated as:

$$E_f = E_{Ce_{1-x}X_xO_2} - E_{CeO_2} + N(E_{Ce} - E_X), \quad (1)$$

with $E_{Ce_{1-x}X_xO_2}$ the total energy of the doped system, E_{CeO_2} the total energy of a bulk CeO_2 supercell without dopants and E_X the bulk energy of the pure solid X = C, Si, Ge, Sn, Pb, Ti, Zr, and Hf. Table 1 shows there to be little or no concentration dependence. A direct comparison to experiment is not straight forward since (1) the calculations do not include temperature and pressure effects and (2) experimental preparation of the samples generally include steps (e.g. thermal treatment) introducing additional free energy into the system making defect formation more likely. However, it is well known that oxygen vacancies form spontaneously in CeO_2 during preparation of the sample,[16] as such, the defect formation energy of oxygen vacancies can be used as reference level. For the PBE functional, the defect formation energy of 1.6% oxygen vacancies in CeO_2 is 3.1 eV.[17,18] This is in reasonable agreement with the values found for bulk reduction (4.65-5.00 eV).[25] Furthermore, Andersson et al. have shown that for DFT+U this vacancy formation energy is lowered, increasing the discrepancy with experiment.[26] Table 1 shows this roughly splits the group IV elements in the group IVa and IVb elements, indicating that the specific electronic structure of the dopant (p-block compared to d-block) may be more important than the dopant oxidation state.[19] It shows that the group IVa elements are "less likely" to form uniformly doped CeO_2, while the group IVb elements are "more likely" to form uniformly doped CeO_2. As such, the former dopants should be considered for applications where surface/interface modifications are persued, while the latter dopants should be better suited for the modification of bulk properties and the formation of solid solutions.

The dopant influence on the bulk modulus B_0 and linear thermal expansion coefficient α_l are calculated for systems with a dopant concentration of 25%. Table 2 shows the distinction between group IVa and IVb dopants. Where the former lead to a decrease in B_0, the latter lead to a slight increase of B_0. In addition, the group IVb dopants show roughly the same B_0 (range <5 GPa), while group IVa dopants give rise to a broader range (50 GPa) of possible B_0 values. On the other hand, the pressure derivative of the bulk modulus B'_0 shows little variation.

Table 1: Defect formation energies (eV) for CeO_2 doping

	PBE			
Dopant element	25%	12.5%	3.704%	3.125%
C	19.687	19.889	19.954	19.967
Si	8.737	8.547	8.530	8.562
Ge	9.495	9.257	9.242	9.254
Sn	7.129	6.967	6.962	6.960
Pb	8.960	8.788	8.777	8.780
Ti	3.454	3.526	3.524	3.532
Zr	0.851	0.884	0.885	0.883
Hf	0.484	0.517	0.517	0.517
Co	11.750	11.780	11.800	11.801
Cu	12.922	12.878	12.878	12.879
Gd	2.396	2.445	2.449	2.448
La	2.437	2.429	2.464	2.469
Nb	4.059	3.746	3.726	3.761
V	6.256	6.320	6.348	6.361
Zn	11.057	11.249	11.282	11.300

Table 2: Calculated equilibrium volume change ΔV_0, bulk modulus B_0, pressure derivative of the bulk modulus B'_0 and linear thermal expansion coefficient at 300 K α_l.

system	ΔV_0 (%)	B_0 (GPa)	B'_0 (-)	α_l (T=300K) (10^{-6} K^{-1})
CeO_2	163.39*	174.2	4.49	11.289
$Ce_{0.75}C_{0.25}O_2$	-3.96	125.5	4.55	17.506
$Ce_{0.75}Si_{0.25}O_2$	-9.18	176.8	4.77	12.745
$Ce_{0.75}Ge_{0.25}O_2$	-6.09	160.1	5.03	15.582
$Ce_{0.75}Sn_{0.25}O_2$	-3.24	172.1	4.65	12.414
$Ce_{0.75}Pb_{0.25}O_2$	0.13	154.3	4.98	15.277
$Ce_{0.75}Ti_{0.25}O_2$	-7.60	185.4	4.46	11.117
$Ce_{0.75}Zr_{0.25}O_2$	-4.62	190.8	4.48	10.522
$Ce_{0.75}Hf_{0.25}O_2$	-5.19	191.0	4.42	10.605
$Ce_{0.75}Co_{0.25}O_2$	-4.60	153.8	3.22	16.969
$Ce_{0.75}Cu_{0.25}O_2$	-2.37	142.1	3.12	14.219
$Ce_{0.75}Gd_{0.25}O_2$	0.28	161.3	4.40	12.067
$Ce_{0.75}La_{0.25}O_2$	3.67	158.0	4.41	11.941
$Ce_{0.75}Nb_{0.25}O_2$	-5.32	190.0	4.44	10.549
$Ce_{0.75}V_{0.25}O_2$	-8.09	182.6	4.53	11.647
$Ce_{0.75}Zn_{0.25}O_2$	-3.18	143.4	4.62	15.227

The linear thermal expansion coefficient at 300 K, shows the group IVb dopants lead only to a marginal decrease of α_l, while group IVa dopants give rise to a significant increase of α_l. Comparison of the bulk modulus and the linear expansion coefficient show them to present an oposite behavior; i.e. if a dopant leads to a decrease of the bulk modulus, it results in an increase of the linear thermal expansion coefficent and vice-verse. This behavior is to be expected, since it can be shown that in the quasi-harmonic approximation:[20]

$$\alpha_l = \frac{\gamma C_V}{3B_0V_0}, \tag{2}$$

with γ the overall Grüneisen parameter and C_V the isochoric heat capacity. For very low dopant concentrations the term $\frac{\gamma C_V}{3V_0}$ can be assumed to be constant leading to an inverse relation between the bulk modulus and the thermal expansion coefficient. Figure 2 shows this inverse relation for the systems with a dopant concentration of 25% discussed in this work. Because of the high dopant concentration the volume contribution in equation 2 can not be considered constant over the entire set of systems, as such it is included in the correlation plot. The solid line indicates a linear fit.

Because the bulk modulus and thermal expansion coefficient have been linked to crack-formation in thin films,[4] and both can be modified through doping, this means that doping can be used to reduce interface strain. Especially in processes where large thermal variations occur it is of interest to try and find materials for which the bulk modulus and thermal expansion coefficient only differ very little, as to provide lattice matching during the whole thermal process. Furthermore, since we already noted that group IVa dopants will lead to surface/interface doping, while group IVb dopants lead to bulk doping, one can easily imagine that combining dopants of both groups might give rise to gradients in the bulk modulus and thermal expansion coefficient, which could be usefull in device applications.

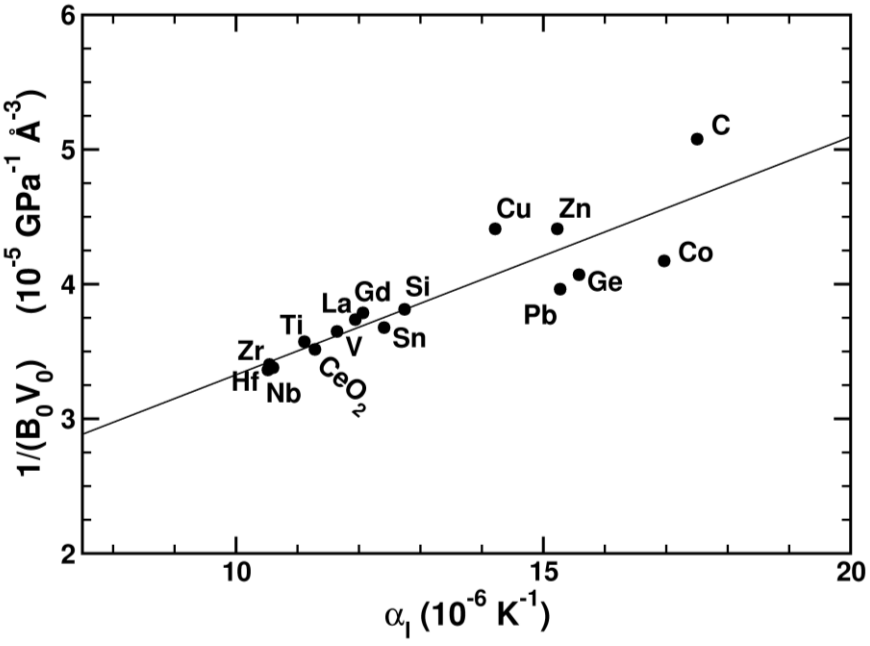

Figure 2: correlation between the linear thermal expansion coefficient α_l and the inverse of the bulk modulus B_0 and equilibrium volume V_0. The solid line indicates a linear fit. Dopant elements are indicated, and CeO_2 indicates the datapoint of the undoped case.

To have a better understanding of how dopants modify the real-space charge distribution, we calculated the Hirshfeld-I charges on the atoms in the systems.[13,14] Since Hirshfeld-I charges are well known to be very transferable,[12] this means they are very well suited to investigate variations in the chemical environment. Table 3 shows the Hirshfeld-I charges for the dopant atoms at different concentrations. The almost immediate convergence of the charges shows us the dopants only have a local influence on the internal charge distribution. This means that simulations on high dopant concentrations have merrit when it is known that experimentally only low dopant concentrations are observed.

Table 3:Concentration dependence of the Hirshfeld-I charges[**] for the group IV dopants in CeO_2.

Dopant element	25%	12.5%	3.704%	3.125%
C	0.96	0.94	0.94	0.94
Si	2.35	2.30	2.30	2.30
Ge	2.35	2.32	2.32	2.33
Sn	2.67	2.64	2.64	2.64
Pb	2.50	2.49	2.49	2.49
Ti	2.66	2.65	2.65	2.65
Zr	2.98	2.98	2.98	2.97
Hf	3.03	3.04	3.04	3.04

Aliovalent Dopants Without Charge Compensating Vacancies

From the previous section, it is already clear that the nature of chemically relevant electrons (p-block versus d-block) has an influence on both stability and mechanical properties of CeO_2. In the following step, we look at the influence of dopants which differ more from Ce, by having a different valence. This different valence in itself also induces the formation of (additional) oxygen vacancies in CeO_2. However, to have a clear view of which part (valence or vacancy) influences the CeO_2 properties in what way, we first investigate CeO_2 systems doped with aliovalent dopants, without the inclusion of oxygen vacancies. In experiments, these systems should be compared to experiments performed under a highly oxidizing atmosphere.

The behavior for the system without oxygen vacancies is quite similar to that of the group IV elements. Some dopant elements are stable (e.g. Lanthanides and Nb) while other are unstable (e.g. Cu[21,22] & Co[23,24], which in experiments are found to form clusters, or high density regions near the grain surface). For the group Vb elements, V and Nb, our simulations show the dopants to present one unpaired electron. Combined with their calculated atomic crystal radius[18] this indicates that these atoms have an oxidation number of IV, meaning that these dopants are interesting aliovalent dopants, which may not induce additional oxygen vacancies. Furthermore, the trend in their formation energy also indicates that Ta is a good candidate to be a stable dopant for CeO_2.

The calculated volumes shown in Table 2 show that only the Lanthanide dopants give rise to a lattice expansion, while other dopants lead to lattice contractions. The calculated bulk moduli on the other hand show that most aliovalent dopants lead to a reduction of the bulk modulus, group Vb elements being the exception. Also the same correlation between the bulk modulus and thermal expansion coefficient is found. In conclusion, behavior observed for the group IV elements is also observed for the aliovalent dopants without vacancies.

Table 4: Influence of Oxygen Vacancies.***

Dopant element	E_f (eV)		B_0 (GPa)		ΔV (%)	
	NV	Vac	NV	Vac	NV	Vac
Cu^{I}	12.922	12.122	142.1	78.6	-2.37	0.88
Zn^{II}	11.057	10.175	143.4	36.3	-3.18	4.13
Gd^{III}	2.396	4.325	161.3	72.4	0.28	3.71

Charge Compensating Vacancies

To investigate the contribution of oxygen vacancies we considered a single oxygen vacancy in the 25% doped systems with Cu^{I}, Zn^{II}, and Gd^{III} doping. Table 4 shows a comparison of systems with and without oxygen vacancy.

The introduction of one oxygen vacancy per dopant atom leads to an improvement of the defect formation energies in case of Cu and Zn. As such, we may expect that doping with these elements will lead to the spontaneous formation of oxygen vacancies. However, the stabilization due to the introduction of the vacancies is insufficient to stabilize these dopants, i.e. to transform them from surface/interface dopants to bulk dopants. In contrast, the introduction of a single vacancy per Gd dopant destabilizes the system. Since Gd has an oxidation number of III, this means that only one vacancy per two Gd dopants is required to have full charge compensation. In the current case vacancy/Gd=1 ratio is too high. As is discussed elsewhere,[18] for a vacancy/Gd ratio of 0.5 the charge compensating vacancy also stabilized the Gd doped system.

In contrast to the defect formation energies, the influence of the charge compensating vacancy on the bulk modulus is large, reducing the bulk modulus by a factor 2 to 4. Altough our simulations use dopant and vacancy concentrations that are much higher than is the case in (most) experiments, this result shows that oxygen vacancies will play a crucial role for bulk-modulus

matching in layered architectures. It shows that the introduction of oxygen vacancies makes CeO_2 less resistant against deformations, which should reduce crack-formation.

Another interesting aspect to the introduction of oxygen vacancies is the resulting increase in system volume. This increase can be sufficient to cancel initial lattice compression due to the introduction of the dopant atoms, as is shown in Table 4. The increase can be understood as a result of the $Ce^{IV} \rightarrow Ce^{III}$ transition. As such, comparing theoretical lattice expansion/contraction with experimental lattice expansion/contraction will always require the inclusion of the experimental concentration of oxygen vacancies in the simulated systems.

CONCLUSIONS

In this work, we study the influence of dopants on the properties of cerium oxide through the use of ab initio calculations. Trends in the stability, lattice parameter, bulk modulus and thermal expansion coefficient of CeO_2 doped with different dopants are investigated. In addition, the influence of charge compensating oxygen vacancies is studied.

We have shown that the valence electron nature plays an important role in the defect stability of the dopant. Using Hirshfeld-I charges it was determined that the modification of the charge redistribution remains localized around the dopant sites. Dopant induced variations of the linear thermal expansion coefficient are shown to be correlated with the inverse of the bulk modulus, allowing to use of one as an indicator for the other.

In contrast to dopants, dopant-vacancy complexes lead to significant modifications of the bulk modulus. The introduction of the charge compensating vacancies makes CeO_2 much less resistant to deformations. In addition, charge compensating vacancies also help stabilizing the defect, showing the introduction of aliovalent dopants will lead to the spontaneous formation of oxygen vacancies. Furthermore, these vacancies also lead to an expansion of the system volume compensating lattice contractions due to the introduced dopant atoms. This shows that oxygen vacancies provide the major contribution to the mechanical and structural modifications of doped CeO_2 systems, while the dopant elements determine the stability of the dopant-vancancy complex.

ACKNOWLEDGEMENTS

This research was financially supported by FWO-Vlaanderen, project no. G. 0802.09N. The computational resources (Stevin Supercomputer Infrastructure) and services used in this work were provided by the VSC (Flemish Supercomputer Center), funded by Ghent University, the Hercules Foundation and the Flemish Government – department EWI.

REFERENCES AND FOOTNOTES

*Equilibrium volume of the cubic CeO_2 12-atom unit cell.

** The Hirshfled-I charges are calculated based on LDA electron densities. It is shown elsewhere, that Hirshfeld-I charges show very little functional independence.

*** NV indicates the system without vacancies, and the relative volume is with regard to the pure CeO_2 system.

[1] Paranthaman, M., Goyal, A., List, F., Specht, E., Lee, D., Martin, P., He, Q., Christen, D., Norton, D., Budai, J., & Kroeger, D. (1997). Growth of Biaxially Textured Buffer Layers on Rolled-Ni Substrates by Electron Beam Evaporation. *Physica C, Volume 275*, 266–272.

[2] Oh, S., Yoo, J., Lee, K., Kim, J. & Youm, D. (1998). Comparative Study on the Crack Formations in the CeO_2 Buffer Layers for YBCO Films on Textured Ni Tapes and Pt Tapes. *Physica C, Volume 308*, 91–98.

[3] Penneman, G., Van Driessche, I., Bruneel, E. & Hoste, S. (2004). Deposition of CeO_2 Buffer Layers and $YBa_2Cu_3O_{7-d}$ Superconducting Layers Using an Aqueous sol-gel Method. *Key Engineering Materials, Volume 264–268*, 501–504.

[4] Van de Velde, N., Van de Vyver, D., Brunkahl, O., Hoste, S., Bruneel, E. & Van Driessche, I. (2010). CeO_2 Buffer Layers for HTSC by an Aqueous Sol-Gel Method – Chemistry and Microstructure. *European Journal of Inorganic Chemistry, Volume 2010*, 233–241.

[5] Narayanan, V., Lommens, P., De Buysser, K., Vanpoucke, D. E. P., Huehne, R., Molina, L., Van Tendeloo, G., Van Der Voort, P. & Van Driessche, I. (2012). Aqueous CSD Approach for the Growth of Novel, Lattice-Tuned $La_xCe_{1-x}O_d$ Epitaxial Layers. *Journal of Materials Chemistry, Volume 22*, 8476–8483.

[6] Blöchl, P.E. (1994). Projector augmented-wave method. *Physical Review B, Volume 50*, 17953–17979.

[7] Kresse, G., & Joubert, D. (1999). From ultrasoft pseudopotentials to the projector augmented-wave method. *Physical Review B, Volume 59*, 1758–1775.

[8] Perdew, J. P., Burke, K., & Ernzerhof, M. (1996). Generalized Gradient Approximation Made Simple. *Physical Review Letters, Volume 77*, 3865–3868.

[9] Maradudin, A. A., Montroll, E. W., Weiss, G. H., & Ipatova, I. P. 1971. "Theory of lattice dynamics in the harmonic approximation," Academic press, New York, 2nd edn.

[10] Vanpoucke, D.E.P. 2011. HIVE 3. http://dannyvanpoucke.be/computational-science-en/

[11] Vinet, P., Smith, J. R., Ferrante, J., Rose, J. H. (1987). Temperature effects on the universal equation of state of solids. *Physical Review B, Volume 35*, 1945–1953.

[12] Bultinck, P., Van Alsenoy, C., Ayers, P. W. & Carbo-Dorca, R. (2007). Critical Analysis and Extension of the Hirshfeld Atoms in Molecules. *Journal of Chemical Physics, Volume 126*, 144111, 9pp.

[13] Vanpoucke, D. E. P., Bultinck, P. & Van Driessche, I. (2013). Extending Hirshfeld-I to Bulk and Periodic Materials. *Journal of Computational Chemistry, Volume 34*, 405–417.

[14] Vanpoucke, D. E. P., Van Driessche, I. & Bultinck, P. (2013). Reply to Comment on "Extending Hirshfeld-I to Bulk and Periodic Materials". *Journal of Computational Chemistry, Volume 34*, 422–427.

[15] Lebedev, V. I., & Laikov, D. (1999). Quadrature Formula for the Sphere of 131-th Algebraic Order of Accuracy. *Doklady Mathematics, Volume 59*, 477–481.

[16] Trovarelli, A. (1996). Catalytic Properties of Ceria and CeO_2-Containing Materials. *Catalysis Reviews: Science and Engineering, Volume 38*, 439–520.

[17] Vanpoucke, D. E. P., Cottenier, S., Van Speybroeck, V., Bultinck, P. & Van Driessche, I. (2012). Tuning of CeO_2 Buffer Layers for Coated Superconductors Through Doping. *Applied Surface Science, Volume 260*, 32–35.

[18] Vanpoucke, D. E. P., Bultinck, P., Cottenier, S., Van Speybroeck, V. & Van Driessche, I. (2014). Aliovalent doping of CeO_2: DFT study of oxidation state and vacancy effects. *Journal of Materials Chemistry A, Volume 2*, 13723-13737.

[19] Vanpoucke, D. E. P., Cottenier, S., Van Speybroeck, V., Van Driessche I. & Bultinck, P. (2014). Tetravalent Doping of CeO_2: The Impact of Valence Electron Character on Group IV Dopant Influence. *Journal of the American Ceramics Society, Volume 97*, 258–266.

[20] Dove, M.T. 1993. "Introduction to lattice dynamics," Cambridge University Press, Camebridge.

[21] Lu, Z., Yang, Z., He, B., Castleton, C. & Hermansson, K. (2011). Cu-doped ceria: Oxygen vacancy formation made easy. *Chemical Physics Letters, Volume 510*, 60–66.

[22] Bera, P., Priolkar, K. R. Sarode, P. R., Hegde, M. S., Emura, S., Kumashiro, R. & Lalla, N. P. (2002). Structural Investigation of Combustion Synthesized Cu/CeO_2 Catalysts by EXAFS and Other Physical Techniques: Formation of a $Ce_{1-x}Cu_xO_{2-\delta}$ Solid Solution. *Chemistry of Materials, Volume 14*, 3591–3601.

[23] Ali, B., Shah, L. R., Ni, C., Xiao, J. Q. & Shah, S. I. (2009). Interplay of dopant, defects and electronic structure in driving ferromagnetism in Co-doped oxides: TiO_2, CeO_2 and ZnO. *Journal of Physics: Condensed Matter, Volume 21*, 456005.

[24] Tiwari, A., Bhosle, V. M., Ramachandran, S., Sudhakar, N., Narayan, J., Budak S., & Gupta, A. (2006). Ferromagnetism in Co doped CeO_2: Observation of a giant magnetic moment with a high Curie temperature *Applied Physics Letters, Volume 88*, 142511.

[25] Panhans, M., & Blumenthal, R. (1993). A Thermodynamic and Electrical Conductivity Study of Nonstoichiometric Cerium Dioxide *Solid State Ionics, Volume 60(4)*, 279–98.

[26] Andersson, D. A., Simak, S. I., Johansson, B., Abrikosov, I. A., & Skorodumova, N. V. (2007). Modeling of CeO_2, Ce_2O_3, and CeO_{2-x} in the LDA + U Formalism *Physical Review B, 75(3)*, 035109.